Journal of Computational Physics 396 (2019) 785–798

Contents lists available at ScienceDirect

Journal of Computational Physics

www.elsevier.com/locate/jcp

Data assimilation for models with parametric uncertainty ☆

Lun Yang [a], Yi Qin [a], Akil Narayan [b], Peng Wang [a,*]

[a] Department of Mathematics and System Sciences, Beihang University, Beijing, 100191, China
[b] Department of Mathematics, and Scientific Computing and Imaging (SCI) Institute, The University of Utah, Salt Lake City, UT, United States of America

ARTICLE INFO

Article history:
Received 25 November 2018
Received in revised form 26 June 2019
Accepted 10 July 2019
Available online 15 July 2019

Keywords:
Particle filter
Data assimilation
Generalized polynomial chaos
Uncertainty quantification
Stochastic Galerkin method
Stochastic collocation method

ABSTRACT

Modeling the behavior of complex systems is notoriously difficult given approximate simulation models, parametric uncertainty, and limited and noisy data. To address such difficulty and harness information from both model forecast and observation, we propose a novel particle filter framework with the generalized polynomial chaos (gPC) method. By constructing a gPC expansion for the system state of interest, our framework delivers a system assimilation procedure that updates gPC coefficients when observations of the system are available, and whose forward model is defined by the stochastic Galerkin method. In this way, one can not only estimate the system state for specific realizations but also its statistical moments, and even the probability density function. The effectiveness of the proposed scheme is demonstrated through four numerical examples.

1. Introduction

Reliable estimates of most physical phenomenon are notoriously elusive due to our incomplete knowledge of the underlying processes and parametric uncertainty within the governing models. Although data acquisition techniques are continuously improving, measurements of system states remain scarce and prone to observational and interpretive errors. Consequently, a robust system simulation must seamlessly combine those two sources of incomplete information.

To address such challenges, one can employ various data assimilation techniques. One popular framework is the Kalman filter [1] and its variants, such as the extended Kalman filer [2,3] and the ensemble Kalman filter [4,5]. These approaches treat both model and measurement errors as Gaussian noise and aim to minimize a quadratic objective through an additive weighting of model forecasts and observations at each assimilation stage. But in practice, most physical systems are nonlinear and their input parameters often exhibit non-Gaussian fluctuations. As a result, the model forecasts are likely to be non-Gaussian.

Alternatively, particle filter strategies [6,7] provide a data assimilation framework for nonlinear system forcasts with arbitrary (non-Gaussian) noise distributions. By employing a finite set of samples (particles) to represent the distribution of system state, a particle filter propagates these particles through the forward model and weighs them through observations

☆ P. Wang, L. Yang and Y. Qin were partially funded by National Key Research and Development Program of China (Grant No. 2017YFB0701700) and the National Natural Science Foundation of China (Grant No. 11571028). A. Narayan was partially supported by AFOSR FA9550-15-1-0467.

* Corresponding author.
E-mail addresses: lun.yang@buaa.edu.cn (L. Yang), akil@sci.utah.edu (A. Narayan), wang.peng@buaa.edu.cn (P. Wang).
URL: http://www.sci.utah.edu/~akil (A. Narayan).

https://doi.org/10.1016/j.jcp.2019.07.020
0021-9991/

at each assimilation stage. However, nonlinearity of the forward model and its parametric uncertainty may render its direct model simulations computationally expensive.

In this paper, we propose a particle filter approach that replaces the forward model with a "cheaper" surrogate model using a generalized polynomial chaos (gPC) expansion [8]. As an extension of classical polynomial chaos theory [9], the gPC method has been widely used in stochastic computation and in many cases is more efficient than direct Monte Carlo simulation (MCS) of nonlinear stochastic system with parametric uncertainty [10]. Earlier works [11,12] have attempted to employ gPC methods in the data assimilation process using an ensemble Kalman filter and Bayesian updates. In contrast, we employ the gPC method in the particle filter framework and update the gPC coefficient system state by assimilating its gPC expansion coefficients with noisy observations.

Our data assimilation framework is formulated in Section 3, which is preceded in Section 2 by a brief summary of gPC methods and the particle filter algorithm. Section 4 investigates the effectiveness of our framework through numerical examples, while key conclusions are drawn in Section 5.

2. Problem setup

In this section, we formulate the general problem of data assimilation and briefly review the basics of generalized polynomial chaos expansions and its major two numerical implementations: the stochastic Galerkin method and the stochastic collocation method. Vectors and matrices are represented by lowercase boldface letters $\mathbf{u}$ and the uppercase boldface letters $\mathbf{U}$, respectively. The matrix transpose of $\boldsymbol{U}$ is denoted by $\boldsymbol{U}^{\mathrm{T}}$ and its inverse is represented by $\boldsymbol{U}^{-1}$.

2.1. Data assimilation

Let $u(\mathbf{x}, t)$ be the "true state" of our system of interest at time $t \in (0, T]$, defined in a physical domain $D \subset \mathbb{R}^{\ell}$, $\ell = 1, 2, 3$, with coordinates $\mathbf{x} = (x_1, ..., x_{\ell})$. To predict the system state at a discrete time step $t \geq 1$, one can approximate its temporal evolution with a forward model $g_{\mathrm{m}}[\cdot]$ that advances a dicretized model state $\boldsymbol{u}$ forward in time:

$$\mathbf{u}(t) = g_{\mathrm{m}}\left[\,\mathbf{u}_{\mathrm{m}}(t-1)\,\right] + \boldsymbol{\epsilon}_{\mathrm{m}}(t). \tag{1}$$

Here, $\mathbf{u}_{\mathrm{m}}(t)$ is the model forecast at the previous time step, and $\boldsymbol{\epsilon}_{\mathrm{m}}(t) \in \mathbb{R}$ represents model error or epistemic uncertainty, which is often assumed as a zero-mean random process in time.

One can estimate the "true state" from observational data ($\mathbf{d} \in \mathbb{R}^{N_{\mathrm{d}}}$, $N_{\mathrm{d}} \geq 1$), which can be sparse and/or incomplete; we let $\mathcal{H}_{\mathrm{d}}$ denote an observation operator that transforms the true state $\mathbf{u}$ into N_{d}-dimensional observational space. Due to uncertainty, such as instrumental and numerical roundoff error, such observation datal may not be exact and often contains an error $\boldsymbol{\epsilon}_{\mathrm{d}}$:

$$\mathbf{d}(t) = \mathcal{H}_{\mathrm{d}}\left[\mathbf{u}(t)\right] + \boldsymbol{\epsilon}_{\mathrm{d}}(t). \tag{2}$$

Here the data error $\boldsymbol{\epsilon}_{\mathrm{d}} \in \mathbb{R}^{N_{\mathrm{d}}}$ is also modeled as a zero-mean random process in time with covariance matrix $\mathbf{D} = \mathbb{E}[\boldsymbol{\epsilon}_{\mathrm{d}}\boldsymbol{\epsilon}_{\mathrm{d}}^{\mathrm{T}}] \in \mathbb{R}^{N_{\mathrm{d}} \times N_{\mathrm{d}}}$. We also note that the operator $\mathcal{H}_{\mathrm{d}}[\cdot]$ can be linear or nonlinear [13]. However, it is commonly treated as linear, e.g. the identity matrix, for simplicity: $\mathcal{H}_{\mathrm{d}}[\cdot] = \mathbf{H} = \mathbf{I}$.

Filtering algorithms are mechanisms that utilize information from both the model forecast $\mathbf{u}_{\mathrm{m}}(t) = g_{\mathrm{m}}\left[\,\mathbf{u}_{\mathrm{m}}(t-1)\,\right]$ and the observational data $\mathbf{d}(t)$, in order to obtain an "analyzed state" $\hat{\mathbf{u}}(t)$ that closely resembles the true system state.

2.2. Generalized polynomial chaos

In practice, the forward model $g_{\mathrm{m}}[\cdot]$ may be numerically difficult to solve and often contains uncertain parameters $\mathbf{z} = \{z_1, \ldots, z_{N_{\mathrm{z}}}\} \in \Omega \subset \mathbb{R}^{N_{\mathrm{z}}}$. Such $\mathbf{z}$-parametric uncertainty is aleatoric uncertainty, whose effect we wish to explicitly model with a forecast. Instead of employing a $\mathbf{z}$-parameterized forward model, one may employ the generalized polynomial chaos (gPC) expansion [14] and construct a N-th order surrogate model $u_N(\mathbf{x}, t, \mathbf{z})$ to approximate the model forecast u_{m}:

$$u_{\mathrm{m}} \approx u_N(\mathbf{x}, t, \mathbf{z}) = \sum_{|\mathbf{i}|=0}^{N} v_{\mathbf{i}}(\mathbf{x}, t)\Psi_{\mathbf{i}}(\mathbf{z}) = \sum_{|\mathbf{i}|=0}^{N} v_{(i_1,\ldots,i_{N_{\mathrm{z}}})}(\mathbf{x}, t)\,\psi_{i_1}(z_1)\cdots\psi_{i_{N_{\mathrm{z}}}}(z_{N_{\mathrm{z}}}), \tag{3}$$

where $\mathbf{i} = (i_1, \ldots, i_{N_{\mathrm{z}}}) \in \mathbb{N}_0^{N_{\mathrm{z}}}$ is a multi-index and $|\mathbf{i}| = i_1 + \cdots + i_{N_{\mathrm{z}}}$. The gPC coefficients are $v_{\mathbf{i}}(\mathbf{x}, t)$, where $\psi_{i_{N_{\mathrm{z}}}}(z_{N_{\mathrm{z}}})$ represents the $i_{N_{\mathrm{z}}}$-th degree orthonormal polynomial associated to the random variable $z_{N_{\mathrm{z}}}$. We assume the random variables $\mathbf{z}$ are mutually independent with known joint distribution $F_{\mathrm{z}}(\mathbf{z}')$ and probability density function $\mathrm{d}F_{\mathrm{z}}$. To facilitate subsequent presentation, we employ the popular *graded lexicographic order* and use a single index to order the summands in the gPC expansion (3).

The multivariate gPC basis $\Psi_{\mathbf{i}}(\mathrm{z})$ are orthonormal polynomials satisfying

$$\mathbb{E}[\Psi_{\mathbf{i}}(\mathbf{z})\Psi_{\mathbf{j}}(\mathbf{z})] = \int_{\Omega} \Psi_{\mathbf{i}}(\mathbf{z}')\Psi_{\mathbf{j}}(\mathbf{z}')\mathrm{d}F_{\mathrm{z}}(\mathbf{z}') = \delta_{\mathbf{i},\mathbf{j}}, \qquad 0 \leq |\mathbf{i}|, |\mathbf{j}| \leq N, \tag{4}$$

where $\delta_{\mathbf{i},\mathbf{j}}$ is the multivariate Kronecker delta function,

$$\delta_{\mathbf{i},\mathbf{j}} = \prod_{d=1}^{N_z} \delta_{i_d,j_d} = \begin{cases} 1 & \text{if} \quad i_d = j_d, \\ 0 & \text{if} \quad i_d \neq j_d. \end{cases} \tag{5}$$

For many distributions of interest, these polynomials can be formed from products of univariate polynomials formed from the Wiener-Askey scheme. In general, the polynomial basis $\{\Psi_{\mathbf{i}}(\mathbf{z})\}$ can be determined from the orthogonality relationship (4). For example, a Gaussian distribution for $\mathbf{z}$ corresponds to tensorized Hermite polynomials while a uniform distribution on a hypercube is related to tensorized Legendre polynomials. Detailed account of hypergeometric polynomials and the Askey scheme can be found in [14–16].

The accuracy of a degree-N truncated gPC method is often measured in the popular L^2-norm, and under some classical approximation theory assumptions one can obtain algebraic convergence with respect to N:

$$\|u_{\mathrm{m}}(\mathbf{z}) - u_N(\mathbf{z})\|^2_{L^2_\Omega} = \int_\Omega |u_{\mathrm{m}}(\mathbf{z}') - u_N(\mathbf{z}')|^2 \mathrm{d}F_z(\mathbf{z}') \leq cN^{-\alpha} \to 0, \qquad N \to \infty. \tag{6}$$

Here $c \in \mathbb{R}$ is constant and $\alpha > 0$ is, informally speaking, a measure on the smoothness of the system state u_{m} as a function of the parameter $\mathbf{z}$. In other words, for a relatively smooth function u_{m}, sufficient accuracy can be achieved with a low-degree gPC expansion u_N.

To create a numerical algorithm that computes coefficients $v_{\mathbf{i}}$ in the gPC expansion (3), one can use either the stochastic Galerkin method (Appendix A) or the stochastic collocation method (Appendix B). Our forecast models will use the stochastic Galerkin method, but one of our assimilation techniques leverages the collocation framework.

3. gPC-based particle filter

In this Section, we present our gPC-based particle filter via two implementations: a "direct" algorithm and a "collocation" algorithm. Our procedure treats the gPC model (A.2a) as a forecast model, and uses observations of the state to update the gPC coefficients in this model. This update is performed via a particle filter.

3.1. Algorithm

The particle filter generates a set of particles (samples) to represent the probabilistic distribution of a system state and weighs them at each time step when data is available. In our gPC-based particle filter, we construct a gPC expansion of the system state to replace the original forward model $g_{\mathrm{m}}[\cdot]$. The system state is updated by its gPC coefficients using the stochastic Galerkin method. Our model forecast (1) becomes:

$$\hat{\mathbf{v}}(t) = g_{\mathrm{N}}[\,\mathbf{v}(t-1)\,] + \boldsymbol{\epsilon}_{\mathrm{N}}(t), \tag{7}$$

where $\hat{\mathbf{v}}$ are the "true" gPC coefficients and $g_{\mathrm{N}}[\cdot]$ is the new forward model defined by the stochastic Galerkin method (A.2a). If one assumes that the model error $\boldsymbol{\epsilon}_{\mathrm{N}}$ is due explicitly to the discrepancy between the exact forward model and the gPC degree-N truncation, then $\boldsymbol{\epsilon}_{\mathrm{N}}(t) = \left(\epsilon_N^{(\mathbf{k})}\right)_{|\mathbf{k}|=0}^{N}$ is given by:

$$\epsilon_N^{(\mathbf{k})}(t) = \epsilon_N^{(\mathbf{k})}(t-1) + \Delta t\, \mathbb{E}\left[\left(\mathcal{L}(u) - \mathcal{L}\left(\sum_{|\mathbf{i}|=0}^{N} v_{\mathbf{i}}(\mathbf{x},t)\Psi_{\mathbf{i}}(\mathbf{z})\right)\right)\Psi_{\mathbf{k}}(\mathbf{z})\right] + \boldsymbol{\epsilon}_{\mathrm{m}}(t)\,\mathbb{E}\left[\Psi_{\mathbf{k}}(\mathbf{z})\right]. \tag{8}$$

Our "direct" algorithm can be summarized as shown in Algorithm 1, which we briefly describe here: Assume that N_c observations of the state u_{m} are available at a parametric ensemble $\left(\mathbf{z}^{(j)}\right)_{j=1}^{N_c}$. As in (B.1a), this results in a vector $\mathbf{u}_{\mathrm{d}}$ serving as the right-hand side of a collocation system. The relation (B.1a) makes clear that the matrix $\boldsymbol{A}$ in this setting is our observation operator $\mathcal{H}_{\mathrm{d}} = \boldsymbol{H}$ in (2). This therefore immediately yields an update through a standard particle filter approach, by considering the discrepancy $\mathbf{u}_{\mathrm{d}} - \boldsymbol{A}\mathbf{v}$, where $\mathbf{v}$ is a forecast. The details are provided in Algorithm 1.

Alternatively, one can employ the following "collocation" algorithm to convert the observations $\mathbf{d} = \mathbf{u}_{\mathrm{d}}$ to gPC coefficients $\mathbf{v}_{\mathrm{d}}$ using stochastic collocation method. The converted "data" will then be assimilated with those from the gPC model. One then performs a standard particle filter update on the collocation estimate of the gPC coefficients. This is detailed in Algorithm 2. In such context, "data" now refers to:

$$\mathbf{d}'(t) = \mathbf{v}_{\mathrm{d}}(t) + \boldsymbol{\epsilon}_{\mathbf{dv}}(t), \tag{9}$$

in which an estimate of the observational error of the gPC coefficients $\boldsymbol{\epsilon}_{\mathbf{dv}} = \left(\epsilon_{\mathrm{d}}^{(\mathbf{k})}\right)_{|\mathbf{k}|=0}^{N}$ can be expressed using a pseudospectral formulation:

Algorithm 1 Direct algorithm.

At time step $n = 0$**:**

- Construct a N-th order gPC expansion of system state $u_{\mathrm{m}}(\mathbf{x}, t, \mathbf{z}) = \sum_{|\mathbf{i}|=0}^{N} v_{\mathbf{i}} \Psi_{\mathbf{i}}(\mathbf{z})$.
- Generate N_{q} sets of particles for the gPC coefficients vector using prescribed distribution and initial values. The particles sets are then assigned with equal weight: $\{\mathbf{v}\}_{k=1}^{N_{\mathrm{q}}} = \left\{ v_0^{(k)}, v_1^{(k)}, \ldots, v_{N_{\mathrm{p}}}^{(k)} \right\}_{k=1}^{N_{\mathrm{q}}}$.

At time step $n \geq 1$**:**

- *Forecast*: estimate the gPC coefficients from previous time step $(n-1)$ using the stochastic Galerkin approach for each set of particles.
- *Importance Sampling*:
  - assign each particle a weight in accordance with the probability density function of the observation noise $\boldsymbol{\epsilon}_{\mathrm{d}}$: $w_n^k \propto P(\mathbf{d}_n | \mathbf{v}_{n|n-1}^k) \propto P(\mathbf{d}_n - \boldsymbol{A}\mathbf{v}_{n|n-1}^k), \quad k = 1, \ldots, N_{\mathrm{q}}$.
  - normalize the particles' weights: $\hat{w}_n^k \leftarrow w_n^k / (\sum_{j=1}^{N_{\mathrm{q}}} w_n^j)$, $k = 1, \ldots, N_{\mathrm{q}}$.
- *Resampling*: resample the N_{q} sets of particles using the discrete probability measure defined by the ensemble $\{\mathbf{v}_{n|n-1}\}_{k=1}^{N_{\mathrm{q}}}$ and its normalized weights $\hat{w}_n^k$, $k = 1, \ldots, N_{\mathrm{q}}$.
  The new sets of particles $\{\mathbf{v}\}_{k=1}^{N_{\mathrm{q}}}$ are then assigned with equal weight for each set.
- *Output*: The gPC coefficients at this time step are: $\mathbf{v}_n = \sum_{k=1}^{N_{\mathrm{q}}} \mathbf{v}_{n|n-1}^k / N_{\mathrm{q}}$.

Algorithm 2 Collocation algorithm.

At time step $n = 0$**:**

- Construct a N-th order gPC expansion of system state $u_{\mathrm{m}}(\mathbf{x}, t, \mathbf{z}) = \sum_{|\mathbf{i}|=0}^{N} v_{\mathbf{i}} \Psi_{\mathbf{i}}(\mathbf{z})$.
- Generate N_{q} sets of particles for the gPC coefficients vector using prescribed distribution and initial values. The particles sets are then assigned with equal weight: $\{\mathbf{v}\}_{k=1}^{N_{\mathrm{q}}} = \left\{ v_0^{(k)}, v_1^{(k)}, \ldots, v_{N_{\mathrm{p}}}^{(k)} \right\}_{k=1}^{N_{\mathrm{q}}}$.

At time step $n \geq 1$**:**

- *Forecast*: estimate the gPC coefficients from previous time step $(n-1)$ using the stochastic Galerkin approach for each set of particles.
- *Measurements*: obtain the gPC coefficients from measurements using stochastic collocation methods as introduced in Appendix B.
- *Importance Sampling*:
  - assign each particle a weight in accordance with the probability density function of the gPC observation noise $\boldsymbol{\epsilon}_{\mathbf{dv}}$: $w_n^k \propto P(\mathbf{v}_{\mathrm{d}} | \mathbf{v}_{n|n-1}^k) \propto P(\mathbf{v}_{\mathrm{d}} - \mathbf{v}_{n|n-1}^k), \quad k = 1, \ldots, N_{\mathrm{q}}$.
  - normalize the particles' weights: $\hat{w}_n^k \leftarrow w_n^k / (\sum_{j=1}^{N_{\mathrm{q}}} w_n^j)$.
- *Resampling*: resample the N_{q} sets of particles using the discrete probability measure defined by the ensemble $\{\mathbf{v}_{n|n-1}^k\}_{k=1}^{N_{\mathrm{q}}}$ and its normalized weights $\hat{w}_n^k$, $k = 1, \ldots, N_{\mathrm{q}}$.
  The new sets of particles are then assigned with equal weight for each set.
- *Output*: The gPC coefficients at this time step are: $\mathbf{v}_n = \sum_{k=1}^{N_{\mathrm{q}}} \mathbf{v}_{n|n-1}^k / N_{\mathrm{q}}$.

$$\epsilon_{\mathrm{d}}^{(|\mathbf{k}|)}(t) = \frac{\sum_{\mathbf{j} > N}^{\infty} \mathbf{u}_{\mathrm{m}}[\Psi_{\mathbf{j}}, \Psi_{\mathbf{k}}]_w}{\mathbb{E}\left[\Psi_k^2(\mathbf{z})\right]} + \sum_{j=1}^{N_{\mathrm{c}}} \boldsymbol{\epsilon}_{\mathrm{d}} \Psi_{\mathbf{k}}(\mathbf{z}^{(j)})\, w_{\mathrm{c}}(\mathbf{z}^{(j)}), \quad |\mathbf{k}| = 1, \ldots, N. \tag{10}$$

Here the first term is also called the aliasing error and $[\cdot, \cdot]_w$ refers to the discrete inner product corresponding to the collocation mesh. In general, the observational error (10) is caused either by the interpolation scheme or the integration rule [10] and can be quantified in some situations.

In essence, the two particle filter schemes differs on their interpretations of what constitutes observations. The direct algorithm utilizes measurements of system state as data in its assimilation procedure. In contrast, the collocation algorithm must convert those measurements of state to "measurements" of the gPC coefficients using the stochastic collocation method. Although it is less straightforward than the direct algorithm and introduces aliasing errors (10), numerical implementations such as compressive sensing may require considerably fewer observations N_{c}.

Two points are also noted here. First, as a particle filter scheme, the initial distribution and values of the gPC coefficients do not affect the assimilation results. Second, the model error of the gPC coefficients (8) consists of two parts, the gPC expansion approximation error and the original forward model error (1). The former error would quickly converge to zero for smooth functions with high order expansions (6), but exact quantification of the forward model error $\boldsymbol{\epsilon}_{\mathrm{m}}$ remains an open question, given that the "true" system state is the unknown quantity of interest, is thus often approximated with ad-hoc experience.

3.2. Theoretical convergence

One can investigate convergence of these approaches using standard particle filter arguments. Following the scheme in [17], let $\boldsymbol{\mu}_n$ be the probability measure at a discrete time step n corresponding to the distribution $P(\mathbf{v}_n | \mathbf{d}_n)$, and $\boldsymbol{\mu}_n^{N_{\mathrm{q}}}$ be its discrete counterpart from N_{q} particles. Assuming existence of a quantity $\kappa \in (0, 1]$:

$$\kappa \leq P(\mathbf{d}_{n+1} | \mathbf{v}_{n+1}) \leq \kappa^{-1}, \quad \forall n \in \mathbb{N}, \tag{11}$$

the "root mean square" distance between the two probability measures can be bounded [17]:

$$\mathrm{dist}(\boldsymbol{\mu}_n^{N_q}, \boldsymbol{\mu}_n) = \sup \sqrt{\mathbb{E}\left[|\boldsymbol{\mu}_n^{N_q} - \boldsymbol{\mu}_n|^2\right]} \leq \sum_{n=1}^{T} (2\kappa^{-2})^n \frac{1}{\sqrt{N_q}} \to 0 \quad \text{as } N_q \to \infty \tag{12}$$

where T is total number of time steps. In other words, the discrete distribution converges to the true distribution as the number of particles increases. For full details on the derivation, refer to [17]. The main question then is the existence of κ and its value; this is problem-specific and is difficult to compute even for concrete examples. However, the purpose of this section is to emphasize that our particle filter approaches can have such convergence statements.

Let us consider a linear model and gaussian noise, so that our assimilation strategy for the mean $\bar{\mathbf{v}}_n = \int \mathbf{v}_n \boldsymbol{\mu}_n(d\mathbf{v}_n)$ is consistent with the results of standard Kalman filter,

$$\bar{\mathbf{v}}_{n+1} = (\mathbf{I} - \mathbf{K}_{n+1}\mathbf{H}) g_N[\bar{\mathbf{v}}_n] + \mathbf{K}_{n+1}\mathbf{d}'_n, \tag{13}$$

where $\mathbf{I}$ is identity matrix and $\mathbf{K}_{n+1}$ is the Kalman gain matrix. If the $\mathbf{K}_{n+1}$ such that $(\mathbf{I} - \mathbf{K}_{n+1}\mathbf{H})g_N$ is globally Lipschitz with constant $\gamma < 1$ in a norm $\|\cdot\|$, then due to theorem 4.10 in [17], the error between the assimilation $\bar{\mathbf{v}}_n$ and the truth $\mathbf{v}_n^t$ satisfies

$$\limsup_{n\to\infty} \|\bar{\mathbf{v}}_n - \mathbf{v}_n^t\| \leq \frac{\beta}{1-\gamma} \max |\, (\boldsymbol{\epsilon}_{\mathrm{dv}})_n \,|, \tag{14}$$

which vanishes as $\max |\, (\boldsymbol{\epsilon}_{\mathrm{dv}})_n \,| \to 0$. Then following the results of (6) & (14), we can obtain the following convergence statement in the L^2_Ω norm by assuming (6).

$$\begin{aligned}
&\|u(\mathbf{z})(\mathbf{x},t) - \sum_{|\mathbf{i}|=0}^{N} \bar{v}_{\mathbf{i}}(\mathbf{x},t)\Psi_{\mathbf{i}}(\mathbf{z})\|^2_{L^2_\Omega} \\
&\leq \|u(\mathbf{z}) - \sum_{|\mathbf{i}|=0}^{N} v^t_{\mathbf{i}}(\mathbf{x},t)\Psi_{\mathbf{i}}(\mathbf{z})\|^2_{L^2_\Omega} + \|\sum_{|\mathbf{i}|=0}^{N} v^t_{\mathbf{i}}(\mathbf{x},t)\Psi_{\mathbf{i}}(\mathbf{z}) - \sum_{|\mathbf{i}|=0}^{N} \bar{v}_{\mathbf{i}}(\mathbf{x},t)\Psi_{\mathbf{i}}(\mathbf{z})\|^2_{L^2_\Omega} \\
&\leq cN^{-\alpha} + \frac{\beta N}{1-\gamma} \max |\, \boldsymbol{\epsilon}_{\mathrm{dv}}(t) \,| \to 0,
\end{aligned} \tag{15}$$

which again vanishes as $N \to \infty$ and $\max |\, (\boldsymbol{\epsilon}_{\mathrm{dv}})_n \,| \to 0$.

4. Numerical examples

In this section, we present various numerical examples to demonstrate the properties of the gPC-based particle filter scheme.

4.1. Ordinary differential equation

Let us first study a linear ordinary differential equation to illustrate the main steps of the gPC-based particle filter:

$$\frac{\mathrm{d}u}{\mathrm{d}t} = -zu, \qquad u(t=0,z) = 1, \quad t \in (0,2], z \in \Omega, \tag{16}$$

in which random parameter z follows a Gaussian distribution $z \sim \mathcal{N}(0, 1^2)$.

We can write its N-th degree gPC expansion as:

$$u(t,z) \approx u_N(t,z) = \sum_{i=0}^{N} v_i(t)\psi_i(z), \tag{17}$$

where $\psi_i(z)$ is the degree-i Hermite polynomial, corresponding to the Gaussian distribution of z.

Following the stochastic Galerkin method, the forward model for the gPC coefficients is:

$$\frac{\mathrm{d}v_k}{\mathrm{d}t}\mathbb{E}\left[\psi_k^2\right] = -v_i \mathbb{E}\left[\sum_{i=0}^{N} z\psi_i\psi_k\right], \quad k = 0, \ldots, N. \tag{18}$$

We also note that the governing equation (16) has an exact solution, $u(t,z) = e^{-zt}$, and its exact gPC expansion coefficients can be found as:

$$\hat{v}_i(t) = \mathbb{E}\left[u(t,z)\,\psi_i(z)\right] = \int_\Omega \mathrm{e}^{-zt}\,\psi_i(z)\frac{1}{\sqrt{2\pi}}\mathrm{e}^{-z^2/2}\mathrm{d}z, \quad i = 0, \ldots, N, \tag{19}$$

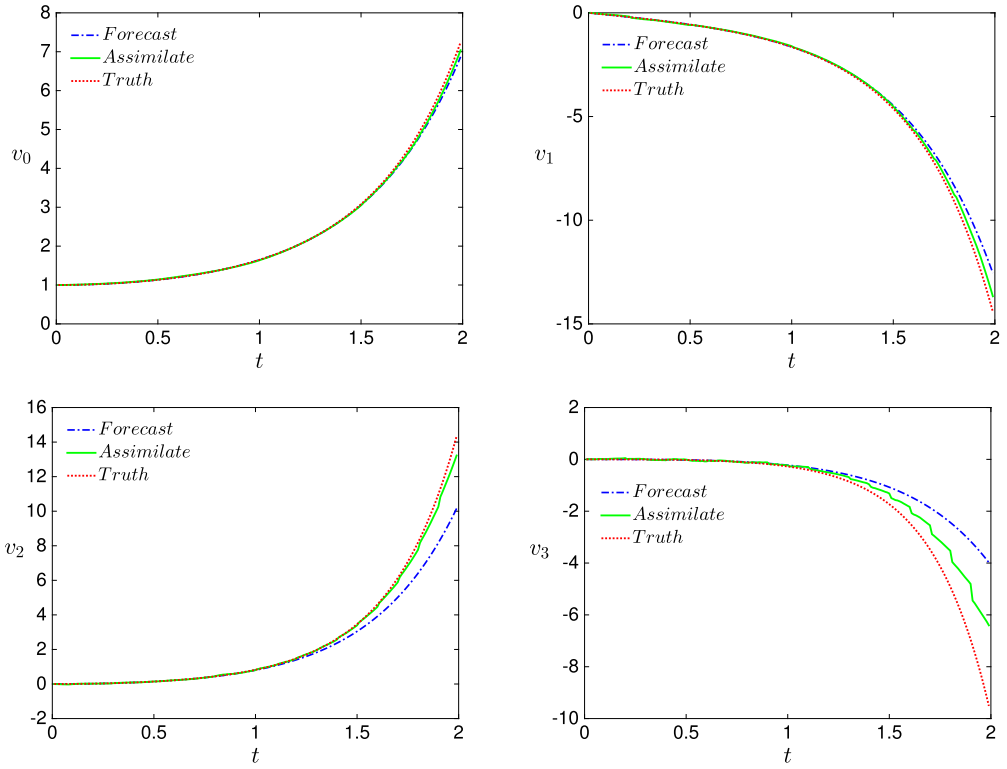

Fig. 1. Temporal evolution of system state's gPC expansion coefficients v_0, v_1, v_2 and v_3, obtained from the forecast model (dash-dot blue line), assimilation (solid green line) and the exact solution (dotted red line). (For interpretation of the colors in the figure(s), the reader is referred to the web version of this article.)

which we use as the "truth" in our analysis.

In the subsequent presentation, we take $N = 3$ for the gPC expansion and compute the forward model (18) for $\mathbf{v} = v_0, v_1, v_2, v_3$ by a fourth-order Runge-Kutta scheme with a time step $\Delta t = 0.01$. The model noise for each gPC coefficients (8) are set as:

$$\epsilon_0 \sim \mathcal{N}(0, 0.02^2), \quad \epsilon_1 \sim \mathcal{N}(0, 0.10^2), \quad \epsilon_2 \sim \mathcal{N}(0, 0.24^2), \quad \epsilon_3 \sim \mathcal{N}(0, 0.34^2), \tag{20}$$

wherein the standard deviations are taken from the mean difference between the model forecast (18) and the exact coefficients (19) over the time domain $[0, 2]$. In total, five hundred observations are computed from the exact solution and are assigned at each assimilation step. They are treated as "perfect" data, i.e. with no observation noise.

We now apply the direct algorithm with an ensemble of $N_q = 500$ particles. Fig. 1 presents the temporal evolution of the gPC expansion coefficients v_0, v_1, v_2, v_3 from the forecast model, assimilation and the exact solution (19), respectively. At each degree, the assimilated coefficients are more accurate than the forecasts; however, as its degree increases, the greater divergence in the model forecast would lead to deterioration in the assimilated results, as shown by the zigzag shape in v_3.

By presenting the system state as a gPC expansion, our proposed particle filter is also capable of computing the probability density function (PDF) of system state. In Fig. 2, we present two snapshots of $P_u(u^*; t)$ at time $t = 0.55$ and $t = 0.65$, computed from model forecast, assimilation and the "truth" solution, respectively. Here new set of observation data were assimilated at $t = 0.61$ between the two snapshots. It is clear that in each snapshot, the assimilated PDF provides a better estimation of the actual solution than direct forecasts. One can also see from the forecast results between the two snapshots that predictions without assimilation would deteriorate over time.

4.2. SIR model

Next, we evaluate our particle filter via a stochastic system of ordinary differential equations, e.g. the susceptible-infected-recovered (SIR) model describing the number of people infected with a contagious illness in a closed population. To be specific, we consider a simplified model, the Kermack-McKendrick model [18], expressed in the following dimensionless form:

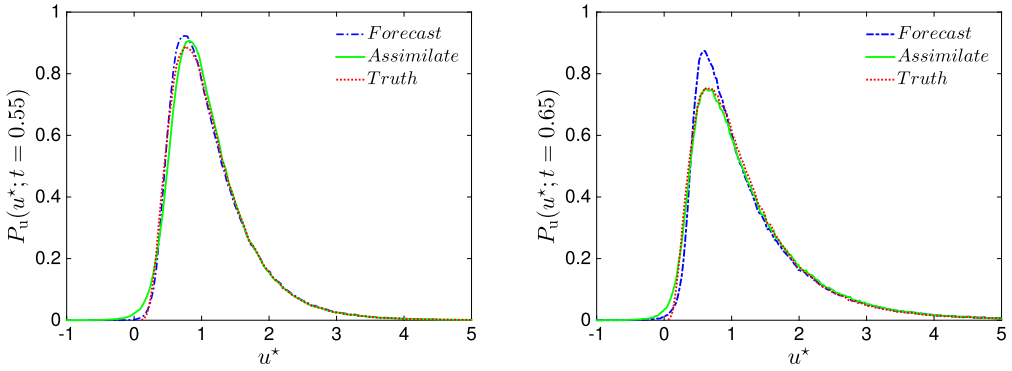

Fig. 2. Snapshots of the probabilistic density function of system state P_u at time $t = 0.55$ and $t = 0.65$, obtained from the forecast model (dash-dot blue line), assimilation (solid green line) and the exact solution (dotted red line), respectively.

$$\frac{dS}{dt} = -\alpha SI, \tag{21}$$

$$\frac{dI}{dt} = \alpha SI - I, \tag{22}$$

$$\frac{dR}{dt} = I, \tag{23}$$

subject to uncertainty in the uniformly-distributed random parameter $\alpha \sim \mathcal{U}[0.1, 10]$ and the following stochastic initial conditions:

$$\begin{cases} S(t=0) \sim \mathcal{U}[0.01, 0.49], \\ I(t=0) \sim \mathcal{U}[0.01, 0.49], \\ R(t=0) \sim \mathcal{U}[0.02, 0.98]. \end{cases} \tag{24}$$

One can see that the SIR model satisfies a conservation law: $S(t) + R(t) + I(t) = 1$. In other words, we can reduce the coupled system of equations to two and the number of random variables to three: $\mathbf{z} = \{\alpha, S(0), I(0)\}$.

Now we construct two N-th order gPC expansions for the system states $S(t, \mathbf{z})$ and $I(t, \mathbf{z})$:

$$S \approx S_N(t, \mathbf{z}) = \sum_{|\mathbf{i}|=0}^{N} \hat{S}_{\mathbf{i}}(t)\Phi_{\mathbf{i}}(\mathbf{z}), \tag{25}$$

$$I \approx I_N(t, \mathbf{z}) = \sum_{|\mathbf{i}|=0}^{N} \hat{I}_{\mathbf{i}}(t)\Phi_{\mathbf{i}}(\mathbf{z}), \tag{26}$$

where $\Phi_{\mathbf{i}}(\mathbf{z})$ are tensorized Legendre polynomials corresponding to the uniform distributions of $\mathbf{z}$.

Following the stochastic Galerkin method, the forward models of the gPC coefficients $\hat{S}_{|\mathbf{k}|}$, $\hat{I}_{|\mathbf{k}|}$, $|\mathbf{k}| = 0, 1, \ldots, N$, are

$$\mathbb{E}\left[\Phi^2_{|\mathbf{k}|}\right]\frac{d\hat{S}_{|\mathbf{k}|}}{dt} = -\sum_{|\mathbf{i}|=0}^{N}\sum_{|\mathbf{j}|=0}^{N} \hat{S}_{|\mathbf{i}|}\hat{I}_{|\mathbf{j}|}\mathbb{E}\left[z_1\Phi_{|\mathbf{i}|}\Phi_{|\mathbf{j}|}\Phi_{|\mathbf{k}|}\right], \tag{27a}$$

$$\mathbb{E}\left[\Phi^2_{|\mathbf{k}|}\right]\frac{d\hat{I}_{|\mathbf{k}|}}{dt} = \sum_{|\mathbf{i}|=0}^{N}\sum_{|\mathbf{j}|=0}^{N} \hat{S}_{|\mathbf{i}|}\hat{I}_{|\mathbf{j}|}\mathbb{E}\left[z_1\Phi_{|\mathbf{i}|}\Phi_{|\mathbf{j}|}\Phi_{|\mathbf{k}|}\right] - \mathbb{E}\left[\Phi^2_{|\mathbf{k}|}\right]\hat{I}_{|\mathbf{k}|}. \tag{27b}$$

In our numerical simulation, the degree of the gPC expansions (25) are set as $N = 8$ and the forward models (27) are solved using a fourth-order Runge-Kutta method with a time step $\Delta t = 0.01$. The same numerical code is exercised on the original equation with 1000 MCS realizations to obtain the "truth" state. To improve our numerical efficiency, we employ hyperbolic cross polynomial space [19], which reduces the total number of coefficients from $\binom{8+3}{3} = 165$ to 44. A Gaussian noise $\mathcal{N}(0, 0.00005^2)$ is prescribed to each gPC coefficients as model forecast error (8) at each time step. The MCS solutions are taken as observation data at each assimilation step but perturbed with Gaussian noise $\mathcal{N}(0, 0.001^2)$.

$N_q = 1000$ sets of particles are employed in the direct algorithm to compute the 44 gPC coefficients. Instead of an exhaustive presentation of all 44 coefficients, we demonstrate the performance of our particle filter in Fig. 3 by the marginal PDFs of the three system states, e.g. P_S, P_I and P_R, at two snapshots: $t = 3.5$ and $t = 5$. Here each snapshot includes PDF solutions from model forecasts, assimilation and the "truth". In general, the assimilated results provide better estimate of the

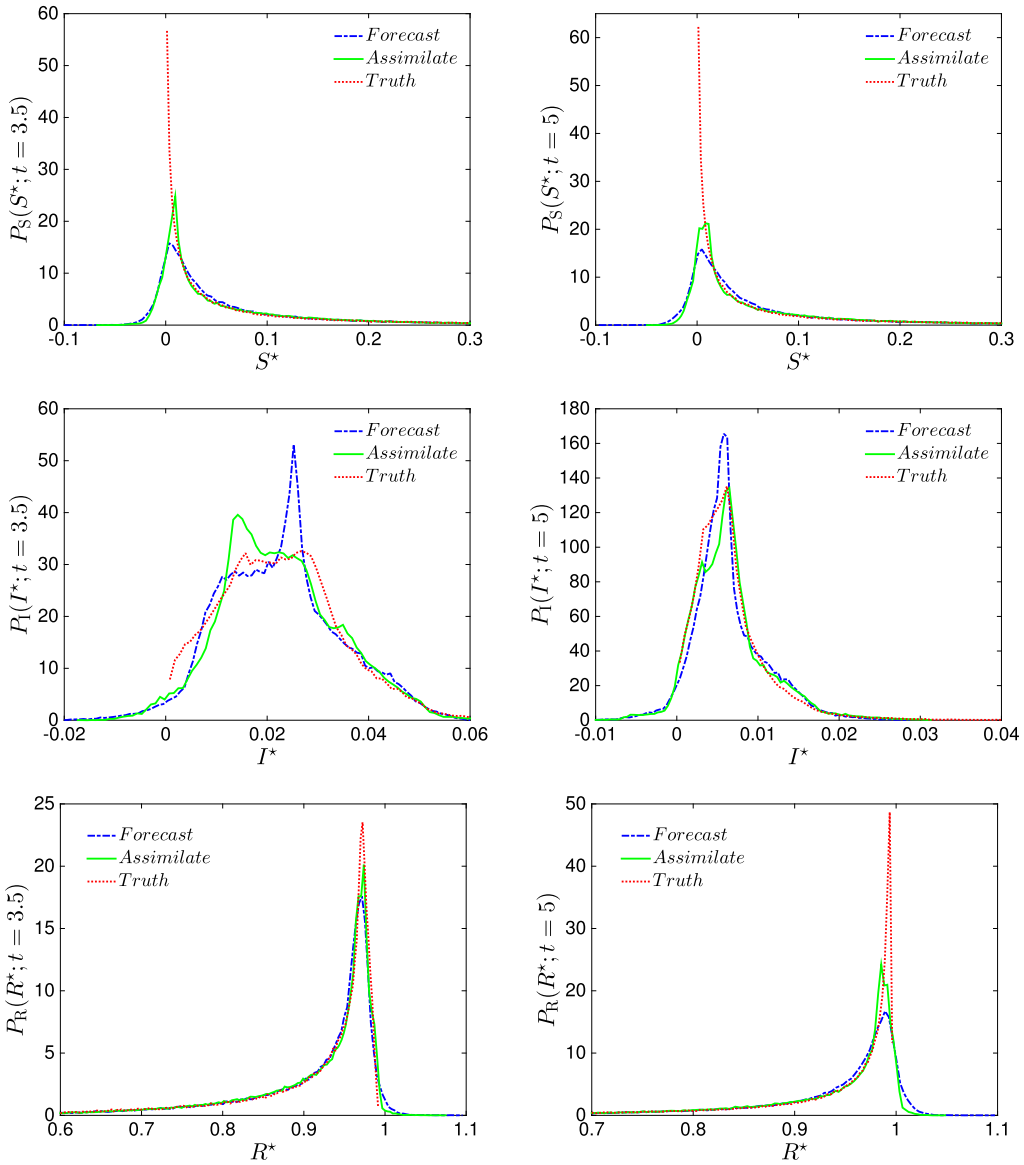

Fig. 3. Snapshots of the marginal PDFs for S, I and R at time $t = 3.5$ and $t = 5$, from model forecast (dash-dot blue line), assimilation (solid green line) and MCS as "truth" (dotted red line), respectively.

"truth" for all three system states at both time. The similarity between $P_S(S^*; t = 3.5)$ and $P_S(S^*; t = 5)$, also indicates that the susceptible population is reaching a steady state. This is expected from SIR model, in which each population group would converge to its steady state albeit at different speed. Discrepancy between assimilation results and the true states may stem from the model forecast errors, which are encapsulated in their unphysical solutions, e.g. $P_S(S^* \leq 0; t) > 0$, $P_I(I^* \leq 0; t) > 0$ and $P_R(R^* \geq 1; t) > 0$. We hope to correct such problems by including physical constrains into the assimilation procedure, which would be the focus of our future work.

4.3. Burgers' equation

We now investigate the performance of our filter scheme on a nonlinear partial differential equation, i.e., viscous Burgers' equation:

$$\frac{\partial u}{\partial t} + \frac{\partial}{\partial x}(0.5u - u^2) = \nu \frac{\partial^2 u}{\partial x^2}, \quad x \in [-3, 3], \tag{28a}$$

$$\begin{cases} u(t, -3) = 0, \quad u(t, 3) = 1 \\ u(0, x) = 0.5 + x/6, \quad x \in [-3, 3] \end{cases} \tag{28b}$$

Here the viscosity ν is a random variable with Gaussian distribution, $\nu \sim \mathcal{N}(\mu_\nu, \sigma_\nu^2)$ and can be further expressed with Reynolds' decomposition:

$$\nu = \mu_\nu + \sigma_\nu z, \quad \text{where} \quad z \sim \mathcal{N}(0, 1^2). \tag{29}$$

By constructing an N-th degree gPC expansion (3) for the system state $u(t, z)$, we find the governing equations of its gPC coefficients v_k, $k = 0, \ldots, N$ using the stochastic Galerkin method:

$$\mathbb{E}\left[\psi_k^2\right] \frac{\partial v_k}{\partial t} = -\frac{\mathbb{E}\left[\psi_k^2\right]}{2} \frac{\partial v_k}{\partial x} + 2 \sum_{i=0}^{N} \sum_{j=0}^{N} v_i \frac{\partial v_j}{\partial x} \mathbb{E}\left[\psi_i \psi_j \psi_k\right] + \sum_{i=0}^{N} \frac{\partial^2 v_i}{\partial x^2} \mathbb{E}\left[\psi_i (\mu_\nu + \sigma_\nu z) \psi_k\right], \tag{30a}$$

which are subject to the following boundary and initial conditions:

$$\begin{cases} v_k(t, -3) = 0, \quad k = 0, \ldots, N \\ v_0(t, 3) = 1, \quad v_i(t, 3) = 0, \quad i = 1, \ldots, N \\ v_0(0, x) = (0.5 + x/6)^2, \quad v_j(0, x) = 0, \quad j = 1, \ldots, N \end{cases}, \tag{30b}$$

where $\psi_k(z)$ is the degree-k Hermite polynomial. We note here the initial condition of the gPC model is deliberately designed as an "incorrect" version of the original condition (28b). It is introduced here to show the robustness of our filter scheme.

In subsequent analysis, we consider a 5th-order gPC expansion and solve the corresponding forward model (30) with a semi-implicit scheme, in which the convective terms and non-linear terms are treated explicitly whilst the viscous terms are computed implicitly [20] with $\Delta x = 0.1875$ and $\Delta t = 0.01$. A Gaussian noise $\sim \mathcal{N}(0, 0.000001^2)$ is introduced to each gPC coefficient forecast as model error (8) at each time step. Monte Carlo simulations (MCS) of 1000 samples are performed on the original system (28) using the same semi-implicit scheme and its solution is considered as "truth". They are then converted to the gPC coefficients for comparison using stochastic collocation methods in Appendix B. The observation data at each assimilation step consists of 200 realizations from the MCS solutions at each spatial point with a random Gaussian error $\sim \mathcal{N}(0, 0.0001^2)$.

Following the direct algorithm (1) with $N_q = 500$ particles, we present solutions of the gPC coefficients $v_0(x, t)$, $v_1(x, t)$, $v_2(x, t)$ and $v_3(x, t)$, obtained from the model forecast, assimilation and truth in Fig. 4 at various space-time points. Although incorrect initial condition (30b) leads to large deviation in the direct model forecast, the assimilation procedure corrects such error and brings the solution closer to its true state.

4.4. Diffusion equation

Lastly, we compare the direct and collocation algorithm via a transient heat conduction system:

$$\frac{\partial u}{\partial t} = \frac{\partial}{\partial x}\left(\alpha(x) \frac{\partial u}{\partial x}\right) + 1, \tag{31a}$$

$$\begin{cases} u(t, -1) = u(t, 1) = 0 \\ u(0, x) = 0 \end{cases}, \qquad (x, t) \in [-1, 1] \times (0, T]. \tag{31b}$$

Here the random model parameter $\alpha(x)$ is the heat conductivity and is treated as a spatially-homogeneous random field. Its mean and two-point covariance are defined as:

$$\mathbb{E}[\alpha] = 10, \quad \mathrm{Cov}_\alpha(x_1, x_2) = e^{-|x_1 - x_2|}. \tag{32}$$

We note the random field can be also expressed by a truncated Karhunen-Loeve expansion (KLE):

$$\alpha(x, \mathbf{z}) \approx \mathbb{E}[\alpha] + \sum_{j=1}^{N_z} \sqrt{\lambda_j} \phi_j(x) z_j. \tag{33}$$

Here $\mathbf{z} = \{z_1, \ldots, z_{N_z}\}$ is a set of mutually-independent random variables with identical uniform distribution over the interval $[-1, 1]$. $\{\lambda_j, \phi_j\}$ are the eigenvalues and eigenfunctions satisfying the integral equations below:

$$\begin{cases} z_j = \frac{1}{\sqrt{\lambda_j}} \int_{-1}^{1} (\alpha(x) - \mathbb{E}[\alpha])\, \phi_j(x) \mathrm{d}x \\ \lambda_j \phi_j(x_1) = \int_{-1}^{1} \mathrm{Cov}_\alpha(x_1, x_2) \phi_j(x_2) \mathrm{d}x_2 \end{cases}, \qquad j = 1, \ldots, N_z. \tag{34}$$

Upon substituting the KLE (33) into (31a), we obtain

$$\frac{\partial u}{\partial t} = \left(\mathbb{E}[\alpha] + \sum_{j=1}^{N_z} \sqrt{\lambda_j} \phi_j z_j\right) \frac{\partial^2 u}{\partial x^2} + \left(\sum_{j=1}^{N_z} \sqrt{\lambda_j} z_j \frac{\partial \phi_j}{\partial x}\right) \frac{\partial u}{\partial x} + 1. \tag{35}$$

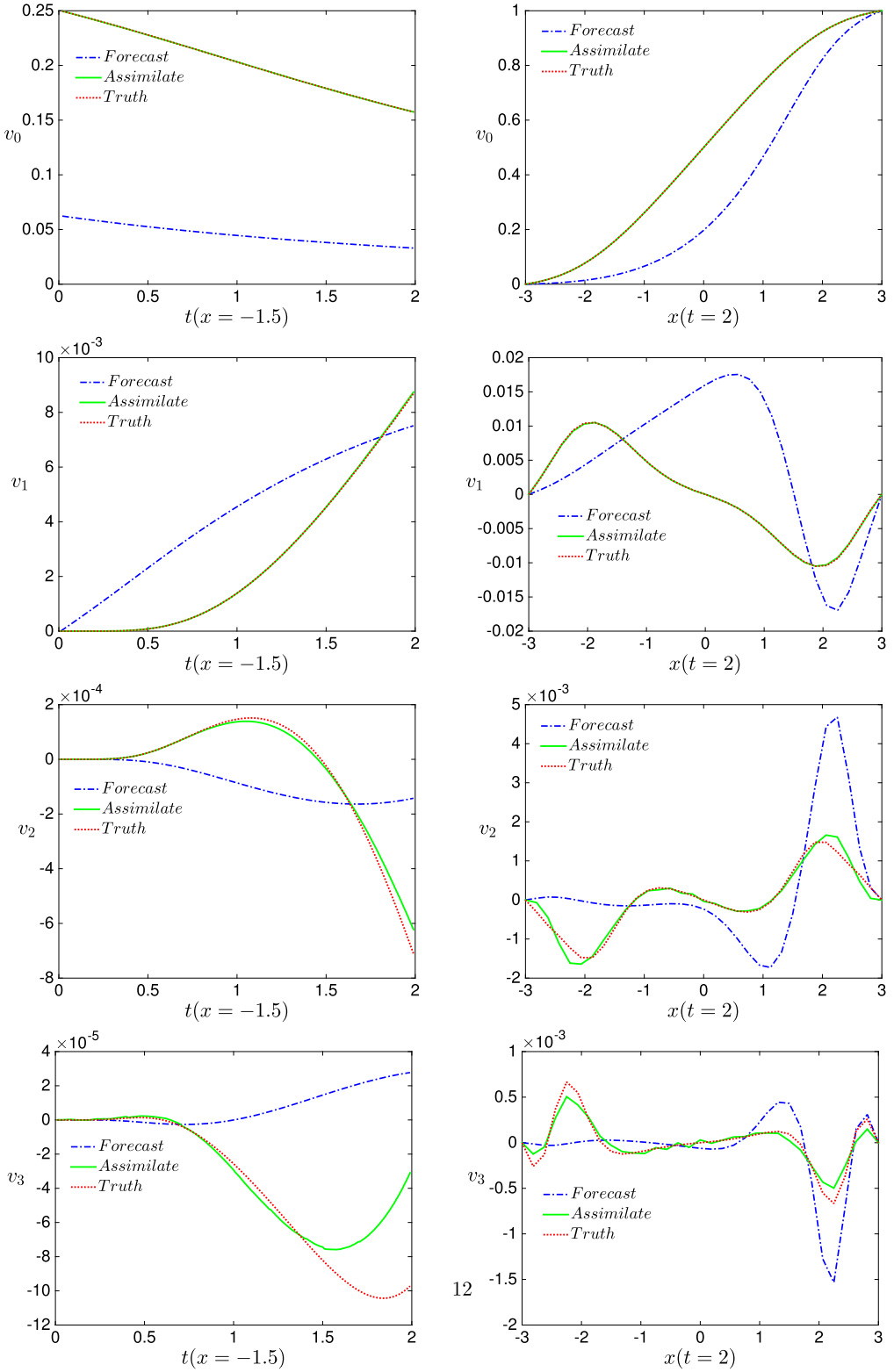

Fig. 4. The temporal and spatial distribution of gPC coefficients $v_0(x,t)$, $v_1(x,t)$, $v_2(x,t)$ and $v_3(x,t)$ as obtained from the forecast model (dash-dot blue line), assimilation (solid green line) and the truth (dotted red line).

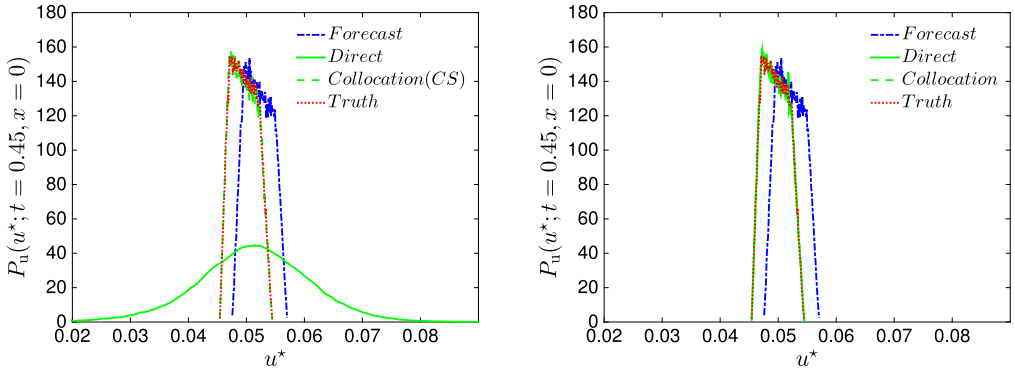

Fig. 5. The system state PDF $P_u(u^\star, x = 0, t = 0.45)$ obtained from Galerkin model (blue dash-dot line), direct algorithm (green line), collocation algorithm (green dashed line) and truth (red dotted line), using two sets of observation data: (a) 42 and (b) 84. Compressive sensing method is employed in the collocation algorithm for the data set 42 while least-square method is applied to the datasets of 84.

By constructing a N-th order gPC expansion: $u \approx \sum_{|\mathbf{i}|=0}^{N} v_{|\mathbf{i}|}(x,t)\Psi_{|\mathbf{i}|}(\mathbf{z})$, one can find its stochastic Galerkin model as:

$$\mathbb{E}\left[\Psi_{|\mathbf{k}|}^2\right]\frac{\partial v_{|\mathbf{k}|}}{\partial t} = \mathbb{E}\left[\Psi_{|\mathbf{k}|}^2\right]\mathbb{E}[\alpha]\frac{\partial^2 v_{|\mathbf{k}|}}{\partial x^2} + \sum_{j=1}^{N_z}\sum_{|\mathbf{i}|=0}^{N}\mathbb{E}\left[\Psi_{|\mathbf{i}|}z_j\Psi_{|\mathbf{k}|}\right]\sqrt{\lambda_j}\phi_j\frac{\partial^2 v_{|\mathbf{i}|}}{\partial x^2}$$
$$+\sum_{j=1}^{N_z}\sum_{|\mathbf{i}|=0}^{N}\mathbb{E}[\Psi_{|\mathbf{i}|}z_j\Psi_{|\mathbf{k}|}\sqrt{\lambda_j}\frac{\partial\phi_j}{\partial x}\frac{\partial v_{|\mathbf{i}|}}{\partial x} + (1+\delta)\mathbb{E}[\Psi_{|\mathbf{k}|}], \quad |\mathbf{k}| = 0, 1, \ldots, N. \tag{36}$$

Here we introduce a deterministic error $\delta \in \mathbb{R} \neq 0$ to the forward model, in order to show the robustness of our filter scheme.

In our simulations, we take $N = 3$ and $N_z = 6$. The "incorrect" forward model (36) ($\delta = 0.05$) is computed with central differencing in space ($\Delta x = 0.1$) and Crank-Nicolson scheme in time ($\Delta t = 0.9\Delta x$). A Gaussian noise $\mathcal{N}(0, 0.002^2)$ is also added to the model forecast at each time step. The same numerical code is employed with MCS to solve the original system (35) with 10^6 realizations, from which the observations are taken as "perfect" data.

We now investigate the effect of observation data size on the assimilation results and compare the two numerical implementations of our gPC-particle filter. To be specific, we present the PDF results at $P_u(u^\star, x = 0, t = 0.45)$ from the "direct" and "collocation" algorithm in Fig. 5 from a) 42 and b) 84 observations at each assimilation stage and for each spatial point. For the collocation algorithm with 42 observations, compressive sampling is used to solve the linear system (B.1a); for 84 observations, (B.1a) is solved in a least squares sense. A total of 2000 particles are employed in both algorithms. It is seen that the collocation algorithm with compressive sensing provides a much better fitting to the "truth" than those from the direct algorithm for a smaller dataset of 42. As the number of observations increases to 84, we employ least-square methods in the collocation algorithm and find that results from the two algorithms are similar to each other; they both agree well with the "true" solution.

This is expected as in "direct" algorithm, difference between "perfect" observation $\mathbf{d}_n$ and the system forecast $\mathbf{A}\mathbf{v}_{n|n-1}^k$, $k = 1, \ldots, N_q$, would be its gPC projection error, $\boldsymbol{\eta} = [\eta_1, ..., \eta_{N_d}]^T \in \mathbb{R}^{N_d}$. If every element of $\boldsymbol{\eta}$ can be assumed as a Gaussian random noise, e.g. $\eta_i \sim \mathcal{N}(0, \sigma_\eta^2)$, $i = 1, .., N_d$, one can rewrite the *Importance Sampling* stage in the "direct" Algorithm 1 as:

$$w_n^k \propto P(\mathbf{d}_n - \mathbf{A}\mathbf{v}_{n|n-1}^k) \propto \exp\left[-\boldsymbol{\eta}\circ\boldsymbol{\eta}/2\sigma_\eta^2\right], \tag{37}$$

where $\circ$ is the Hadamard (componentwise) product.

Meanwhile, by employing least-square method in the "collocation" algorithm, e.g. : $\mathbf{v}_d = \left(\mathbf{A}^T\mathbf{A}\right)^{-1}\mathbf{A}^T\mathbf{d}_n$, and taking its interpolation error as Gaussian noise, e.g. $\boldsymbol{\epsilon}_{\mathbf{dv}} \sim \mathcal{N}(0, \sigma_{\mathbf{dv}}^2)$, the *Importance Sampling* stage in the "collocation" Algorithm 2 becomes:

$$w_n^k \propto P(\mathbf{v}_d - \mathbf{v}_{n|n-1}^k) \propto \exp\left[-\left(\mathbf{v}_d - \mathbf{v}_{n|n-1}^k\right)\circ\left(\mathbf{v}_d - \mathbf{v}_{n|n-1}^k\right)/2\sigma_{\mathbf{dv}}^2\right]$$
$$= \exp\left\{-\left[\left(\mathbf{A}^T\mathbf{A}\right)^{-1}\mathbf{A}^T\left(\mathbf{d}_n - \mathbf{A}\mathbf{v}_{n|n-1}^k\right)\right]\circ \left[\left(\mathbf{A}^T\mathbf{A}\right)^{-1}\mathbf{A}^T\left(\mathbf{d}_n - \mathbf{A}\mathbf{v}_{n|n-1}^k\right)\right]/2\sigma_{\mathbf{dv}}^2\right\}. \tag{38}$$

Comparing (37) and (38), one can see that the two algorithms would be equivalent if the following condition is met:

$$\sigma_d^{-1} = \left[\left(\mathbf{A}^T\mathbf{A}\right)^{-1}\mathbf{A}^T\right]\sigma_{\mathbf{dv}}^{-1}. \tag{39}$$

Although not included here, one can also show equivalence between the two algorithms should an alternative collocation method (such as compressive sensing) be used.

5. Conclusion

In this paper we developed a data assimilation scheme for stochastic systems with parametric uncertainty. Based on the framework of particle filter, we construct generalized polynomial chaos (gPC) expansions to represent the system states and derive forward models for its gPC coefficients with the stochastic Galerkin method. By doing so, the system states can be thus predicted via updating its gPC coefficients. At the time when observations are available, the coefficients can be then assimilated using one of the two implementations of the particle filter, the direct algorithm or collocation algorithm, respectively. Through four numerical examples, our study leads to the following conclusions:

- The proposed scheme provides better prediction of the stochastic system states than direct model forecast. It is robust even if its forward models of gPC coefficients are flawed, such as low gPC order, incorrect model expression or initial conditions.
- By assimilating its gPC expansion coefficients, our scheme is also capable of updating statistical moments of the system states, and can even compute its probability density function.
- Larger set of observation data would improve the accuracy of the proposed scheme.
- The collocation algorithm of proposed scheme requires less observation data than the direct algorithm, albeit additional effort must be made to convert measurements of system state to "measurements" of gPC coefficients via the stochastic collocation method.
- The proposed scheme can be further improved should model error be better quantified and physical constrains be included. This is the focus of future work.

Appendix A. The stochastic Galerkin method

The stochastic Galerkin (SG) method is an extension of the classical Galerkin approach for deterministic equations. With $\mathbb{P}_N^{N_z}$ the space of N_z-variate polynomials of degree N or less, the SG method seeks a solution in the polynomial space $\mathbb{P}_N^{N_z}$ such that residual of the forward model is orthogonal to the polynomial space $\mathbb{P}_N^{N_z}$.

Let us consider the following forward model:

$$\frac{\partial u_{\mathrm{m}}}{\partial t} = \mathcal{L}(u_{\mathrm{m}}, \mathbf{z}), \qquad D \times (0,T] \times \Omega, \tag{A.1a}$$

$$\begin{cases} \mathcal{B}(u_{\mathrm{m}}) = 0, & \partial D \times [0,T] \times \Omega, \\ u_{\mathrm{m}} = u_0, & D \times \{t=0\} \times \Omega, \end{cases} \tag{A.1b}$$

where $\mathcal{L}(\cdot)$ is an operator, $\mathcal{B}(\cdot)$ is a boundary condition operator and u_0 is the initial condition.

Substituting the gPC expansion (3) into the forward model (A.1a) and multiplying with $\Psi_{\mathbf{k}}(\mathbf{z})$, $|\mathbf{k}| = 0, 1, \ldots, N$, respectively, we then take expectations at both sides of the equation:

$$\mathbb{E}\left[\sum_{|\mathbf{i}|=0}^{N} \frac{\partial v_{\mathbf{i}}}{\partial t}\Psi_{\mathbf{i}}(\mathbf{z})\Psi_{\mathbf{k}}(\mathbf{z})\right] = \mathbb{E}\left[\mathcal{L}\left(\sum_{|\mathbf{i}|=0}^{N} v_{\mathbf{i}}(\mathbf{x},t)\Psi_{\mathbf{i}}(\mathbf{z})\right)\Psi_{\mathbf{k}}(\mathbf{z})\right], \quad D \times (0,T] \times \Omega, \tag{A.2a}$$

$$\begin{cases} \mathbb{E}\left[\mathcal{B}\left(\sum_{|\mathbf{i}|=0}^{N} v_{\mathbf{i}}\Psi_{\mathbf{i}}(\mathbf{z})\right)\Psi_{\mathbf{k}}(\mathbf{z})\right] = 0, & \partial D \times [0,T] \times \Omega \\ \mathbb{E}\left[\sum_{|\mathbf{i}|=0}^{N} v_{\mathbf{i}}(\mathbf{x},0)\,\Psi_{\mathbf{i}}(\mathbf{z})\Psi_{\mathbf{k}}(\mathbf{z})\right] = \mathbb{E}[u_0\Psi_{\mathbf{k}}(\mathbf{z})], & D \times \{t=0\} \times \Omega \end{cases}. \tag{A.2b}$$

Based on the form of $\mathcal{L}$ and using the orthogonality relationship (4), we can evaluate the expectation operator $\mathbb{E}(\cdot)$ in (A.2a) and arrive with a system of $N_{\mathrm{p}} = \binom{N+N_z}{N}$ coupled equations for the gPC coefficients $v_{\mathbf{i}}$. While this introduces additional computational expense as N_z becomes large, the gPC formulation for some systems of interest with very large N_z can achieve high levels of accuracy with a feasible number of degrees of freedom [21,22].

Appendix B. The stochastic collocation method

The stochastic collocation method is a popular choice for complex systems where well-established deterministic codes are available. It seeks a solution such that the residual of the forward model (A.1a) is zero at a set of discrete nodes, e.g. the $\mathbf{z}$-collocation points. In other words, if one obtains an ensemble of observations, $\{u_{\mathrm{d}}^{(j)}\}_{j=1}^{N_{\mathrm{c}}}$, at the nodes $\{\mathbf{z}^{(j)}\}_{j=1}^{N_{\mathrm{c}}}$, the gPC expansion (3) would lead to a set of N_{c} equations:

$$\mathbf{A}^{\mathrm{T}}\mathbf{v} = \mathbf{u}_{\mathrm{d}}, \tag{B.1a}$$

$$\mathbf{A} = \left(\Psi_{\mathbf{k}}(\mathbf{z}^{(j)})\right), \quad 0 \le |\mathbf{k}| \le N,\ 1 \le j \le N_{\mathrm{c}}, \tag{B.1b}$$

$$\mathbf{v} = \begin{pmatrix} v_1 \\ \vdots \\ v_{N_{\mathrm{p}}} \end{pmatrix}, \quad \mathbf{u}_{\mathrm{d}} = \begin{pmatrix} u_{\mathrm{d}}(\mathbf{x}, t, \mathbf{z}^{(1)}) \\ \vdots \\ u_{\mathrm{d}}(\mathbf{x}, t, \mathbf{z}^{(N_{\mathrm{c}})}) \end{pmatrix}. \tag{B.1c}$$

Here $\mathbf{A}$ is the Vandermonde-like coefficient matrix, $\mathbf{v}$ is the (unknown) coefficient vector, and $\mathbf{u}_{\mathrm{d}}$ is the observation vector at the collocation points.

Unless $N_{\mathrm{c}} = N_{\mathrm{p}}$ and $\mathbf{A}$ is full rank, such system of equations cannot be uniquely satisfied and specific strategies are required to implement the stochastic collocation method:

- $N_{\mathrm{c}} > N_{\mathrm{p}}$: the system (B.1a) is overdetermined and can be solved by a least-squares method [23].
- $N_{\mathrm{c}} = N_{\mathrm{p}}$: the system is square and potentially invertible, assuming the geometric configuration of the samples $\{\mathbf{z}^{(j)}\}_{j=1}^{N_{\mathrm{c}}}$ avoids certain pathological arrangements. In general one can avoid such pathologies by resorting to unisolvent strategies such as least orthogonal interpolation [24].
- $N_{\mathrm{c}} < N_{\mathrm{p}}$: the system is underdetermined but one can seek a unique and sparsest solution via compressive sampling [25–27].

A more detailed description on how the gPC coefficients are computed in these cases can be found at [28]. Yet another alternative is a pseudospectral approach, which is applicable regardless of the value of the ratio $N_{\mathrm{c}}/N_{\mathrm{p}}$. In essence, the gPC expansion coefficients are computed using an N_{c}-point quadrature rule:

$$w_{\mathbf{i}} = \frac{\mathbb{E}[\Psi_{\mathbf{i}}(\mathbf{z})\mathbf{u}_{\mathrm{d}}(\mathbf{z})]}{\mathbb{E}[\Psi_{\mathbf{i}}^2(\mathbf{z})]} = \frac{\sum_{j=1}^{N_{\mathrm{c}}} \Psi_{\mathbf{i}}(\mathbf{z}^{(j)})\,\mathbf{u}_{\mathrm{d}}(\mathbf{z}^{(j)})\,w_{\mathrm{c}}(\mathbf{z}^{(j)})}{\mathbb{E}[\Psi_{\mathbf{i}}^2(\mathbf{z})]}, \tag{B.2}$$

where locations and weights $w_{\mathrm{c}}(\mathbf{z}^{(j)})$ of the collocation points are predetermined once the quadrature rule and its level are selected. For high-dimensional random parameters, tools like sparse grids [29] are popular in reducing the overall computational costs.

References

[1] R.E. Kalman, et al., A new approach to linear filtering and prediction problems, J. Basic Eng. 82 (1) (1960) 35–45.
[2] A.H. Jazwinski, Stochastic Processes and Filtering Theory, vol. 64, Academic Press, 1970.
[3] A. Gelb, Applied Optimal Estimation, MIT Press, 1974.
[4] G. Evensen, Sequential data assimilation with a nonlinear quasi-geostrophic model using Monte Carlo methods to forecast error statistics, J. Geophys. Res., Oceans 99 (C5) (1994) 10143–10162.
[5] G. Evensen, Data Assimilation: The Ensemble Kalman Filter, Springer Science & Business Media, 2009.
[6] A. Doucet, S. Godsill, C. Andrieu, On sequential Monte Carlo sampling methods for Bayesian filtering, Stat. Comput. 10 (3) (2000) 197–208.
[7] M.S. Arulampalam, S. Maskell, N. Gordon, T. Clapp, A tutorial on particle filters for online nonlinear/non-Gaussian Bayesian tracking, IEEE Trans. Signal Process. 50 (2) (2002) 174–188.
[8] D. Xiu, G.E. Karniadakis, The Wiener–Askey polynomial chaos for stochastic differential equations, SIAM J. Sci. Comput. 24 (2) (2002) 619–644.
[9] R.G. Ghanem, P.D. Spanos, Stochastic Finite Elements: A Spectral Approach, Courier Corporation, 2003.
[10] D. Xiu, Numerical Methods for Stochastic Computations, Princeton University Press, Princeton, New Jersey, 2010.
[11] J. Li, D. Xiu, A generalized polynomial chaos based ensemble Kalman filter with high accuracy, J. Comput. Phys. 228 (15) (2009) 5454–5469.
[12] M. Arnst, R. Ghanem, C. Soize, Identification of Bayesian posteriors for coefficients of chaos expansions, J. Comput. Phys. 229 (9) (2010) 3134–3154.
[13] F. Rabier, Overview of global data assimilation developments in numerical weather-prediction centres, Q. J. R. Meteorol. Soc. 131 (613) (2005) 3215–3233, https://doi.org/10.1256/qj.05.129. URL http://onlinelibrary.wiley.com/doi/10.1256/qj.05.129/abstract.
[14] D. Xiu, G. Karniadakis, The Wiener-Askey polynomial chaos for stochastic differential equations, SIAM J. Sci. Comput. 24 (2) (2002) 619–644.
[15] W. Schoutens, Stochastic Processes and Orthogonal Polynomials, Springer-Verlag, New York, 2000.
[16] R. Koekoek, R. Swarttouw, The Askey-Scheme of Hypergeometric Orthogonal Polynomials and Its q-Analogue, Tech. Rep. 98-17, Department of Technical Mathematics and Informatics, Delft University of Technology, 1998.
[17] K. Law, A. Stuart, K. Zygalakis, Data Assimilation: A Mathematical Introduction, vol. 62, Springer, 2015.
[18] W.O. Kermack, A.G. McKendrick, A contribution to the mathematical theory of epidemics, Proc. R. Soc. Lond., Ser. A, Math. Phys. Eng. Sci. 115 (772) (1927) 700–721, https://doi.org/10.1098/rspa.1927.0118, http://rspa.royalsocietypublishing.org/content/115/772/700.full.pdf. URL http://rspa.royalsocietypublishing.org/content/115/772/700.
[19] J. Bäck, F. Nobile, L. Tamellini, R. Tempone, Stochastic spectral Galerkin and collocation methods for PDEs with random coefficients: a numerical comparison, in: Spectral and High Order Methods for Partial Differential Equations, Springer, 2011, pp. 43–62.
[20] D. Xiu, G.E. Karniadakis, Supersensitivity due to uncertain boundary conditions, Int. J. Numer. Methods Eng. 61 (12) (2004) 2114–2138.
[21] A. Cohen, R. DeVore, C. Schwab, Convergence rates of best N-term Galerkin approximations for a class of elliptic sPDEs, Found. Comput. Math. 10 (6) (2010) 615–646, https://doi.org/10.1007/s10208-010-9072-2. URL https://link.springer.com/article/10.1007/s10208-010-9072-2.
[22] C. Schwab, C.J. Gittelson, Sparse tensor discretizations of high-dimensional parametric and stochastic PDEs, Acta Numer. 20 (2011) 291–467, https://doi.org/10.1017/S0962492911000055.
[23] A. Cohen, M.A. Davenport, D. Leviatan, On the stability and accuracy of least squares approximations, Found. Comput. Math. 13 (5) (2013) 819–834, https://doi.org/10.1007/s10208-013-9142-3. URL http://link.springer.com/article/10.1007/s10208-013-9142-3.

[24] A. Narayan, D. Xiu, Stochastic collocation methods on unstructured grids in high dimensions via interpolation, SIAM J. Sci. Comput. 34 (3) (2012) A1729–A1752, https://doi.org/10.1137/110854059. URL http://epubs.siam.org/doi/abs/10.1137/110854059.
[25] A. Doostan, H. Owhadi, A non-adapted sparse approximation of PDEs with stochastic inputs, J. Comput. Phys. 230 (8) (2011) 3015–3034, https://doi.org/10.1016/j.jcp.2011.01.002. URL http://www.sciencedirect.com/science/article/pii/S0021999111000106.
[26] H. Rauhut, R. Ward, Sparse Legendre expansions via ℓ_1-minimization, J. Approx. Theory 164 (5) (2012) 517–533, https://doi.org/10.1016/j.jat.2012.01.008.
[27] L. Yan, L. Guo, D. Xiu, Stochastic collocation algorithms using l1-minimization, Int. J. Uncertain. Quantificat. 2 (3) (2012) 279–293, https://doi.org/10.1615/Int.J.UncertaintyQuantification.2012003925. URL http://www.dl.begellhouse.com/journals/52034eb04b657aea,3495dd1f6253a653,1447d224370655d6.html.
[28] A. Narayan, T. Zhou, Stochastic collocation on unstructured multivariate meshes, Commun. Comput. Phys. 18 (01) (2015) 1–36, https://doi.org/10.4208/cicp.020215.070515a, arXiv:1501.05891 [math.NA]. URL http://journals.cambridge.org/article_S181524061500047X.
[29] H.-J. Bungartz, M. Griebel, Sparse grids, Acta Numer. 13 (1) (2004) 147–269, https://doi.org/10.1017/S0962492904000182. URL http://journals.cambridge.org/action/displayAbstract?fromPage=online&aid=227245.